

Synthesis of Bioconjugated *sym*-Pentasubstituted Corannulenes: Experimental and Theoretical Investigations of Supramolecular Architectures

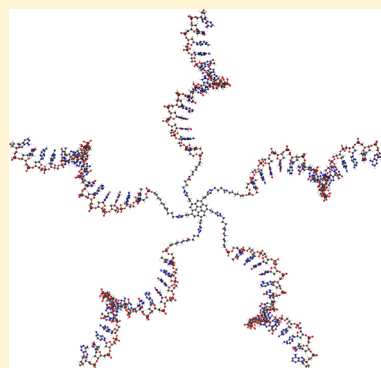
Martin Mattarella,[†] Laura Berstis,[†] Kim K. Baldrige,^{*,†} and Jay S. Siegel^{*,†,‡}

[†]Institute of Organic Chemistry, University of Zurich, Winterthurerstrasse 190, 8057 Zurich, Switzerland

[‡]School of Pharmaceutical Science and Technology, Tianjin University, A203/Building 24, 92 Weijin Road, Nankai District, Tianjin, 300072 P. R. China

Supporting Information

ABSTRACT: Applications of supramolecular architectures span a broad range of fields from medicinal chemistry to materials science and gas storage, making the design and synthesis of such structures a goal of high interest. The unique structural and symmetric properties of corannulene and the recent synthetic developments of C_5 -symmetric pentafunctionalized derivatives motivate efforts to synthesize bioconjugated-corannulene systems and investigate their supramolecular assembly properties. Herein is presented the synthesis of *sym*-pentasubstituted corannulenes functionalized with sugar (galactose and ribose), oligopeptide, nucleosides (thymidine and deoxyadenosine), and palindromic oligonucleotide strands. Experimental and theoretical results demonstrate capability of supramolecular assembly formation in these constructs. Ab initio theoretical modeling enables further evaluation of structure and energetics of oligonucleotide-functionalized corannulene formation. Results indicate formation of aggregates, although icosahedral supramolecular formation is not observed. Analyses suggest future improvements to synthetic routes to achieve icosahedral architectures.



INTRODUCTION

Controlled preparation of three-dimensional (3D) architectures is an important and long-standing goal in the field of supramolecular chemistry, with diverse applications as scaffolds for molecular organization,¹ gas storage materials,² drug delivery vehicles,^{3,4} templates for the development of new materials,⁵ and tools for encapsulating and controlling reactivity of guest molecules.^{6–8} A number of methods for the formation of noncovalent nanostructure have been developed,^{9–22} with promising results from amphiphilic bioconjugates functionalized with oligopeptides,^{23–29} nucleosides,^{30–33} and carbohydrates.^{34–36} Pioneering results reported by Seeman et al.^{37–40} show the potential of annealing complementary DNA strands as a high-specificity approach to preparing nano-objects with desired structures and symmetry.

Molecular building blocks with fivefold symmetry offer the potential of forming icosahedral supramolecular assemblies.⁴¹ Such icosahedra are common in structural biological and in inorganic clusters;^{42–44} however, the directed supramolecular synthesis of such structures from organic building blocks remains a challenging target. In this regard, the high-symmetry and geometrical properties of C_5 -symmetric pentasubstituted derivatives of corannulene, **1**, make supramolecular aggregates of this class of compounds an attractive option.

Besides icosahedral aggregates, the supramolecular chemistry of corannulene bioconjugates could lead to several new materials. In particular, the curved geometry of the aromatic

core imparts a relatively high dipole moment to the molecular and different electronic properties on the concave vs convex π -face.⁴⁵ Columnar architectures from derivatives of **1** have been observed in solid^{46–50} and liquid-crystalline phases,⁵¹ and shown to respond to an electric field and display ferroelectric properties.^{51–55}

Recently, a kilogram-scale synthesis of **1** was developed,⁵⁶ which allowed the investigation of synthetic routes to *sym*-pentachlorocorannulene, **2**,⁵⁷ on a 20 g scale. From **2**, a general strategy via Fe-catalyzed cross coupling chemistry made available a large family of fivefold symmetric penta-functionalized corannulene derivatives, on a scale of hundreds of milligrams, displaying virtually any of the functional groups common in organic chemistry.⁵⁸

The synthesis of *sym*-pentabioconjugated corannulene derivatives functionalized with lipids⁵⁹ and (oligo)-saccharide^{58,60} has been achieved with a copper-catalyzed alkyne–azide cycloaddition reaction (CuAAC) on penta-terminal acetylene corannulene derivative **3** (Figure 1). These promising results motivated the present elaboration of a general strategy to *sym*-pentabioconjugated corannulene derivatives, and investigation of their assembling behavior. The geometric properties of single-stranded DNA (ssDNA) conjugated

Received: September 5, 2013

Revised: December 3, 2013

Published: December 9, 2013

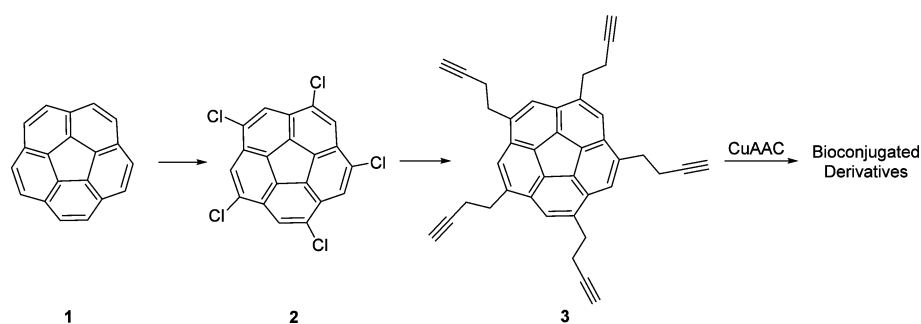
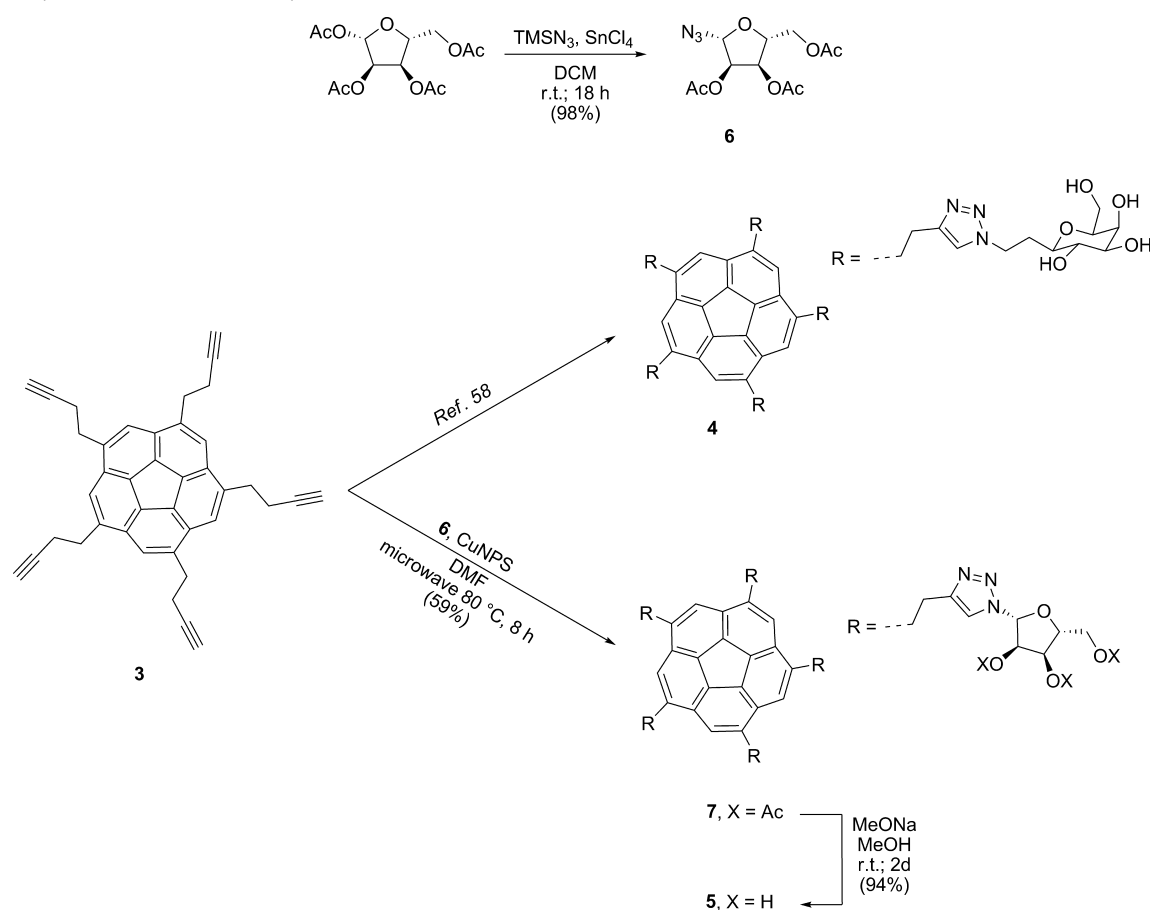


Figure 1. Synthetic route for the synthesis of fivefold symmetric pentabioconjugated corannulene.

Scheme 1. Synthesis of Pentakis-Glycoside Corannulene Derivatives, 4, 5, and 7



corannulene is also computationally characterized with a new implementation of semiempirical *ab initio* methodology, supporting the experimental findings and offering suggestions for improved molecular design in future constructs.

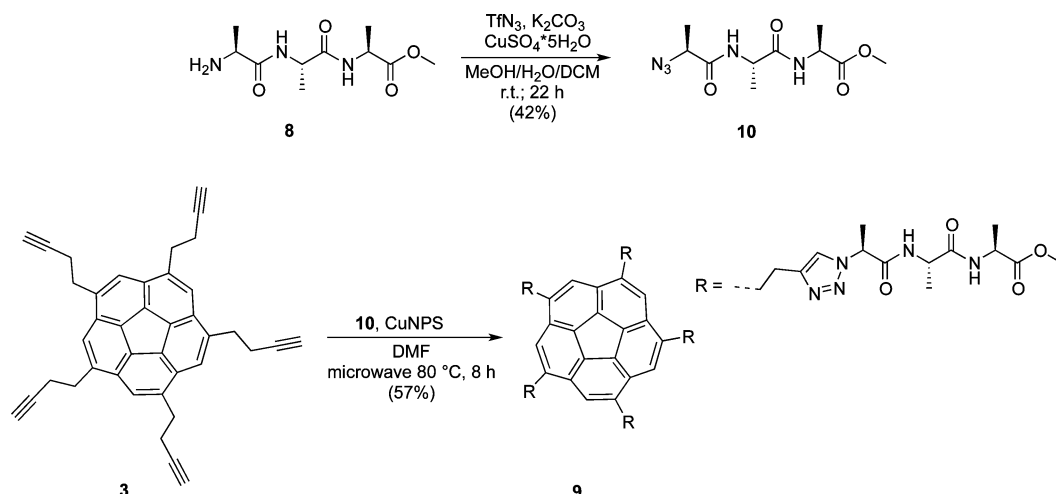
Design and Synthesis. Many intermolecular interactions are involved in the formation of supramolecular aggregates of amphiphilic molecules, including dipole–dipole, π – π stacking, hydrogen bonding, nonspecific van der Waals, hydrophobic, electrostatic, and repulsive steric interactions. Energetic stabilization from a combination of these forces counterbalance the entropic cost of desolvation and polymolecular aggregation.²⁴ Based on these concepts, three classes of C_5 -symmetric pentabioconjugated corannulene derivatives functionalized with carbohydrate, oligopeptide, and nucleoside were designed and synthesized.

In the first class of pentakis-carbohydrate corannulene derivatives, galactoside **4**⁵⁸ and riboside **5** were chosen. Two different moieties in its structure offer possible modes of interaction: the hydrophobic aromatic core, enabling π – π interactions, and the five hydrophilic sugar units surrounding the corannulene, which direct columnar organization in water via the hydrophobic effect.⁶¹

The synthesis of *sym*-pentariboside corannulene **5** was achieved with a CuAAC reaction of the alkyne **3** with 2,3,5-tri-*O*-acetyl- β -D-ribofuranosyl-1-azide **6**⁶² yielding the peracetylated corannulene derivative **7** which was subsequently deprotected with sodium methoxyde (Scheme 1).

Compound **5** was obtained in good yield and in high purity. With azides present on the secondary carbon,^{58–60} such as in **6**, it was observed that the CuAAC reaction required a higher temperature (80 °C) and longer reaction time (8 h) in order to

Scheme 2. Synthesis of Pentakis-Oligopeptide Corannulene, 9



achieve full conversion of the starting material, perhaps due to steric hindrance to accessing the azide group. The protection of the hydroxyl groups of ribose was necessary for the high-purity isolation of compound 7 from the crude mixture.

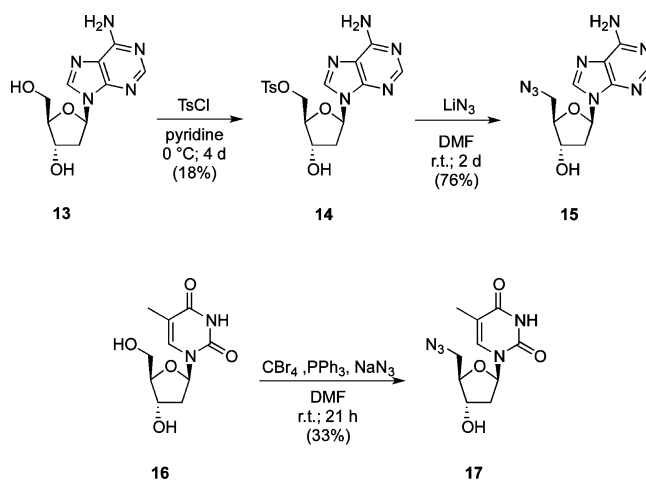
For the second class of bioconjugated pentapods, a corannulene core was functionalized with the tripeptide H-Ala-Ala-Ala-OMe, **8**. This oligopeptide was selected due to its capability to form β -strands in solution,^{63,64} and therefore its potential to utilize H-bonding networks to form interesting and intricate supramolecular structures in solution. For instance, dimeric or polymeric columnar assemblies of the corannulene core could be stabilized by H-bonds between the oligopeptide chains.

Corannulene derivative **9** was prepared in good yield and high purity via the CuAAC reaction of alkyne **3** with the azide derivative **10**, which was prepared by treatment of the amine **8** with triflyl azide prepared in situ (Scheme 2). As for the synthesis of **7**, a higher temperature (80 °C) and longer reaction time (8 h) was required.

Nucleosides are an important class of biomolecules that forms strong and predictable intermolecular H-bonding networks through Watson and Crick base pairing. These interactions can both drive and stabilize the formation of C_5 -symmetric dimers of complementary base-pair *sym*-pentasubstituted corannulene derivatives, utilizing either adenine-thymine (A-T) or cytosine-guanine (C-G) pairing. For this third class of bioconjugated corannulene in the present work, the base-pair A-T was selected, and pentakis-thymidine **11** and pentakis-deoxyadenosine corannulene **12** derivatives were synthesized starting from **3** and the azido-nucleosides **17** and **15**. Preparation of 5'-azido-2'-deoxy-adenosine **15** was achieved by nucleophilic substitution of 5'-tosylated-2'-deoxy adenosine **14**⁶⁵ with lithium azide. The relatively low yield obtained for the synthesis of compound **14** by reaction of **13** with tosyl chloride was due to the formation of 2'-tosylated and 5'-3'-ditosylated products. The 5'-azido thymidine **17** was synthesized following a reported⁶⁶ one-step procedure, reacting thymidine **16** with carbon tetrabromide, triphenylphosphine, and sodium azide (Scheme 3).

Fivefold symmetric pentabioconjugated corannulene derivatives **11** and **12** were synthesized in good yield and high purity with a CuAAC reaction of alkyne **3** and azides **17** and **15**, respectively (Scheme 4).

Scheme 3. Synthesis of Azido-Nucleosides Derivatives, 15 and 17



The successful synthesis of these bioconjugated pentapods^{58–60} demonstrates the robustness and applicability of the CuNPS-catalyzed CuAAC procedure for the preparation of new classes of C_5 -symmetric pentafunctionalized corannulene derivatives.

Capitalizing on the bowl-shaped geometry and C_5 -symmetry of *sym*-pentasubstituted corannulene derivatives, the synthesis of icosahedral supramolecular aggregates was approached using DNA-based bioconjugation, which offers high specificity for formation of highly symmetric structures. Four general strategies for construction of 3D DNA-based architecture have been developed. The first strategy, “DNA origami”, involved the folding of a long single-stranded DNA (ssDNA) into the designed geometry by annealing with short “staple strands”.⁶⁷ This procedure enables high geometrical control,^{68–73} but requires the use of hundreds of different staple strands, as well as a long assembly time. The second strategy involves the use of identical branched DNA building blocks that assemble into DNA cages that present only dsDNA and a defined symmetry.^{74,75} The third strategy, developed by Sleiman, is based on the assembly of ssDNA polygons with organic corner units, which are then assembled by ligation into 3D DNA architectures.^{76–80} This strategy has been improved and simplified by development of a procedure in which the

Scheme 4. Synthesis of Azido-Nucleosides Derivatives, 11 and 12

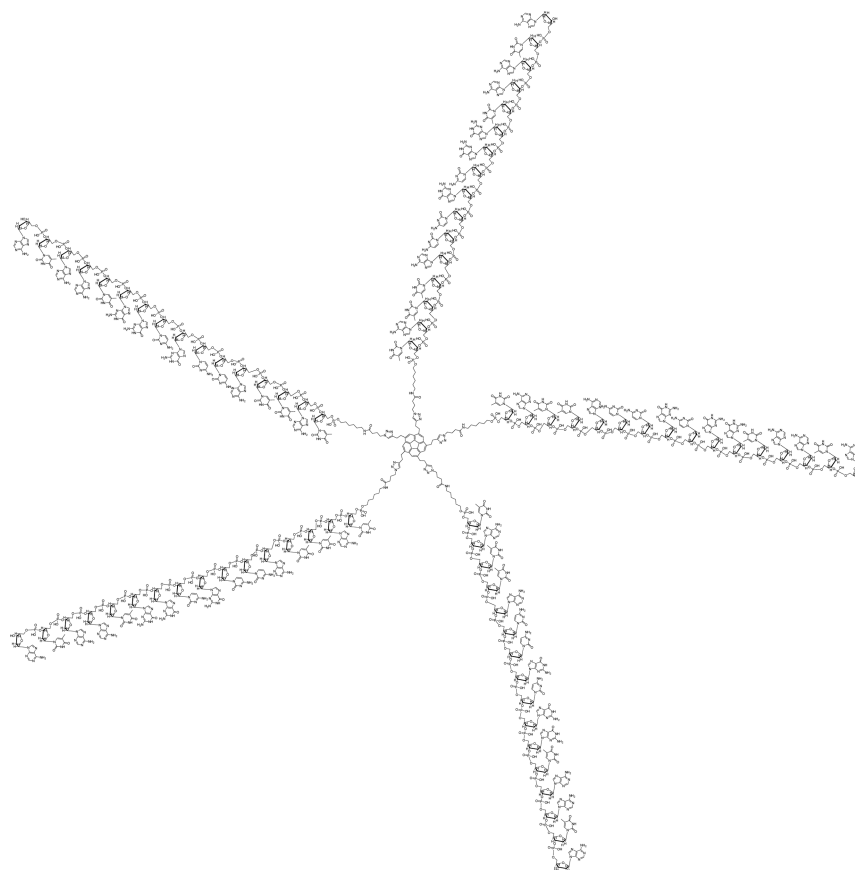
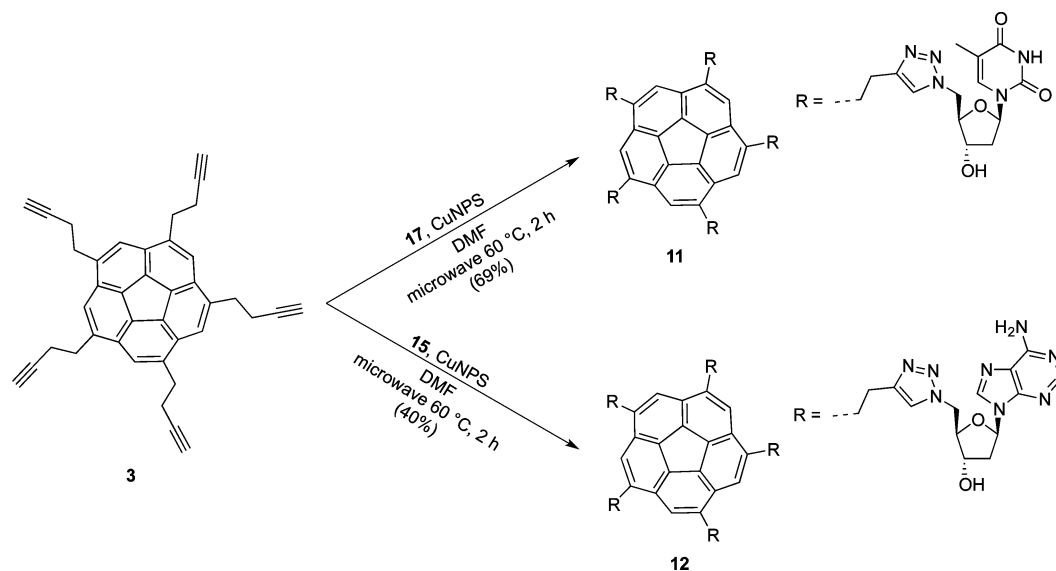


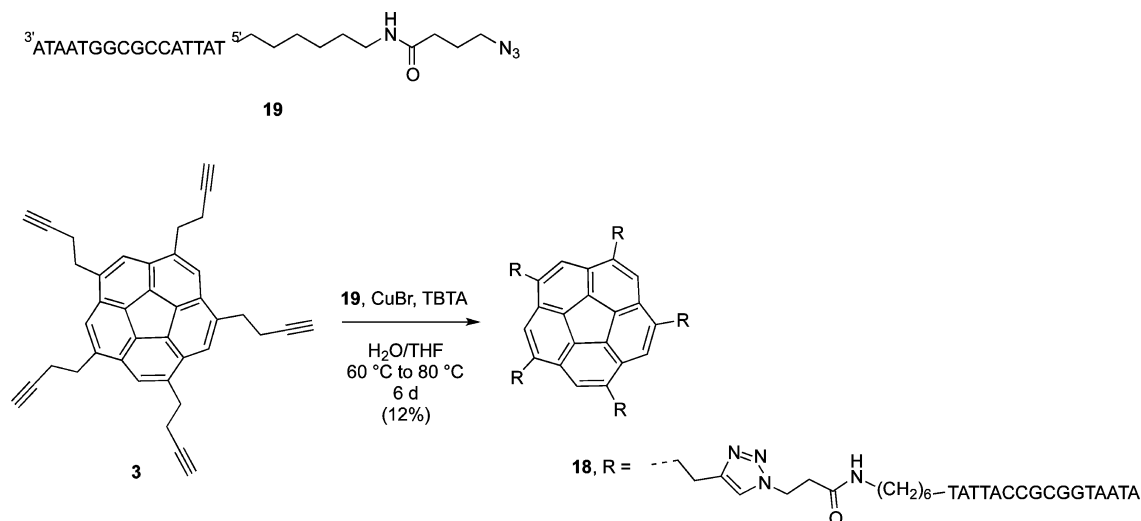
Figure 2. Pentakis-DNA corannulene, 18.

DNA polygon is formed without the separate ligation step.⁸¹ The fourth approach, developed by von Kiedrowski, involves formation of a fully dsDNA 3D-architecture via annealing poly-DNA-functionalized organic molecules.^{82,83}

In the present work, the fourth strategy was chosen for formation of icosahedral aggregates, since coupling the bioconjugation to an organic corannulene core was an important component. The structure of the pentakis-DNA corannulene **18** was designed to utilize a 16-base self-

complementary ssDNA sequence (Figure 2), with high concentration of T and A at the 5'- and 3'-end, to avoid the formation of loops, and a central C/G region to increase the stability of the double-stranded structure. As such, the ssDNA chains may fully anneal with the ssDNA strands of other molecules in solution into many polymeric structures, including a supramolecular icosahedral capsid.

Compound **18** was synthesized by a CuAAC “click” reaction of the alkyne **3** with the 5'-alkylazido-modified oligonucleotide

Scheme 5. Synthesis of *sym*-Pentaoligonucleotide Corannulene 18

19. Since the oligonucleotide **19** is not stable under the conditions of a CuNPS-catalyzed CuAAC reaction, a new synthetic procedure was developed for the functionalization of compound **3**. After screening of several conditions, the best results in terms of yield and time were obtained using copper(I) bromide as the copper source together with *tris*-(benzyltriazolymethyl)amine (TBTA)⁸⁴ as a ligand and stabilizer of Cu (I) species in a mixture of THF and water (Scheme 5).

RESULTS AND DISCUSSION

Due to the hydrophobic corannulene core of the amphiphilic sugar pentapods, **4** and **5**, combined with the strongly hydrophilic galactoside and riboside functionalization, these molecules may form stacked supramolecular aggregates in aqueous solution. Unfortunately, riboside corannulene **5** did not show any solubility in water, but was only soluble in strongly polar solvent such as DMF and DMSO. Therefore, formation of aggregates in water was investigated only for galactoside, **4**, via ¹H NMR, absorption, and emission spectroscopy.

The thermodynamic behavior of the aggregation phenomena was evaluated by means of ¹H NMR spectral analysis for several solutions of **4**, across a range of concentrations and temperatures. Upon increasing the temperature of a solution at constant concentration of **4**, a downfield progression of the chemical shift (δ_{obs}) of the five homotopic hydrogens atoms on corannulene core was observed (Figure 3).

The association constants, K_a , associated with the aggregation of **4** in water were calculated as a function of temperature by nonlinear least-squares regression based on the equal K or isodesmic (K_E) model of indefinite self-association, as described by Martin (Figure 4).⁸⁶

K_a -values (Table 1) were obtained by fitting the experimental data to eq 1, where δ_{obs} is the observed chemical shift, δ_{mon} is the chemical shift of monomer, K_a is the association constant, c is the molar concentration of the sample, and Δ is the difference in the chemical shift of the monomer and the aggregate.

$$\delta_{\text{obs}} = \delta_{\text{mon}} - \Delta \left\{ 1 + \frac{[1 - \sqrt{(4K_a c + 1)}]}{2K_a c} \right\} \quad (1)$$

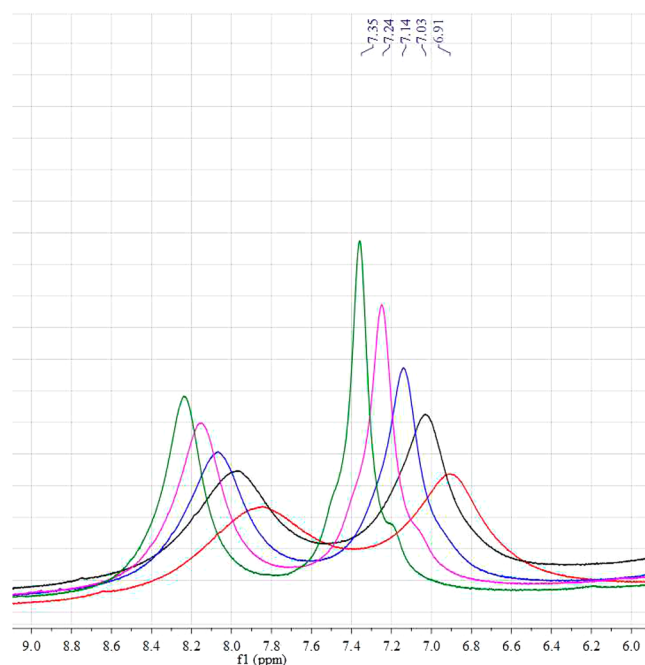


Figure 3. Aromatic region of ¹H NMR spectra of a solution 0.28 mM of **4** at 300 K (red), 310 K (black), 320 K (blue), 330 K (violet), and 340 K (green); δ_{obs} of corannulene hydrogens are shown. Chemical shifts of the water peak at each temperature were calculated in previous work.⁸⁵

The aggregation number N , i.e., the number of the monomers included in the aggregates, was determined using eq 2, where N is the aggregation number. An aggregation number of 2 was estimated with the assumption that **4** is in equilibrium between the monomer and the aggregate.^{87,88}

$$\ln[c(\delta_{\text{mon}} - \delta_{\text{obs}})] = N \ln[c(\delta_{\text{obs}} - \delta_{\text{agg}})] + \ln K_a + \ln N - (N - 1) \ln(\delta_{\text{mon}} - \delta_{\text{agg}}) \quad (2)$$

The thermodynamic parameters, ΔH (-13 ± 1 kcal mol⁻¹) and ΔS (-18 ± 4 cal mol⁻¹), associated with the dimerization process, were determined with a Van't Hoff plot of the K_a values calculated at various temperatures (Figure 5). Surprisingly, unlike most amphiphilic molecules, the driving force for

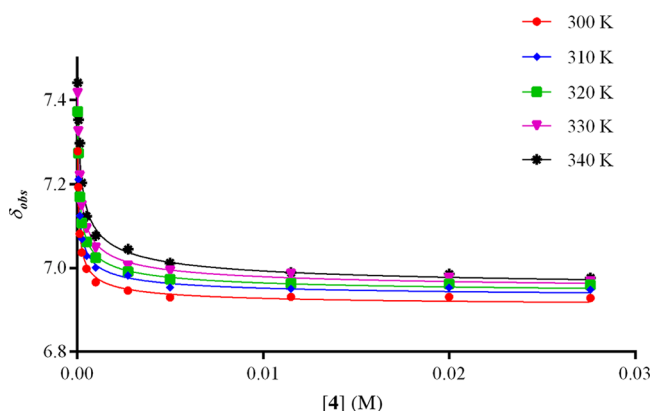


Figure 4. Fitted curves of ^1H NMR spectra of **4**.

Table 1. Association Constant K_a for the Aggregation of **4** at Different Temperatures

T (K)	K_a ($\times 10^4$) (M^{-1})
300	20 ± 10
310	5 ± 2
320	6 ± 2
330	3 ± 1
340	1.4 ± 0.3

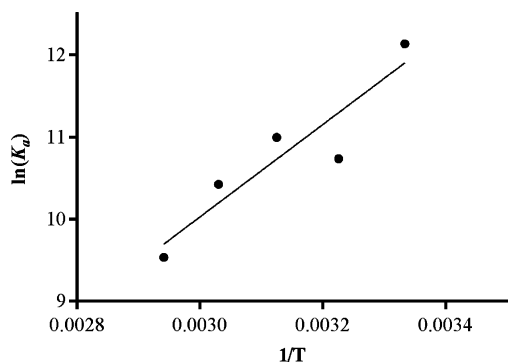


Figure 5. Van't Hoff plot for compound **4**.

aggregation of **4** in solution is not the increase in entropy of the system, but the exothermicity of the process.

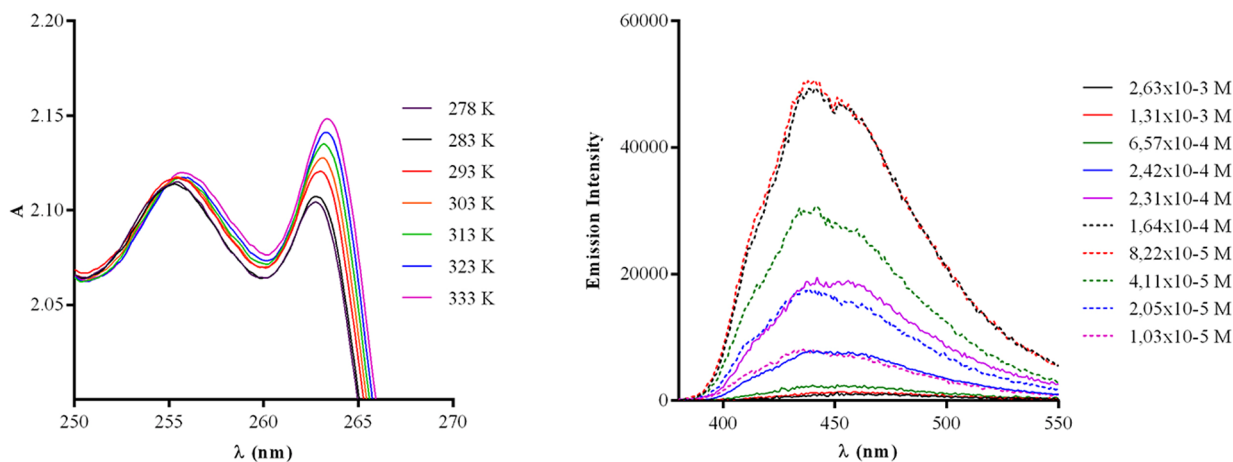


Figure 6. Selected region of UV spectra of a solution of **4** at varying temperature (left). Emission spectra of solution of **4** at varying concentrations (right).

The hypsochromic shift in the absorption spectra as a function of increasing temperature (Figure 6, left) and the quenching of the fluorescence due to the increasing of the concentration of **4** (Figure 6, right) suggest formation of H-dimers in solution.^{89,90} CD analysis of the aggregation process did not show any significant signal in the range of the investigated concentration, because of the low signal-to-noise ratio obtained at these conditions.

Poor solubility of corannulene derivatives **9**, **11**, and **12** in nonpolar organic solvents did not permit investigation of formation of supramolecular assemblies from these compounds through formation of H-bonding networks. These bioconjugated compounds are highly soluble in strong polar solvents such as DMF, DMSO, and TFE. However, ^1H NMR and UV-vis investigation of solutions of **9**, **11**, and **12** in these solvents did not substantiate formation of any aggregates. Most probably, the absence of supramolecular constructs is due to the saturation of the H-bonding sites by the solvent.

Formation of aggregates was further investigated by HR-MS measurements; the high sensitivity of this technique enables study of highly diluted solution of compounds **9**, **11**, and **12** in methanol. While the pentakis-oligopeptide, **9**, did not show formation of any aggregates, the MS spectrum of a solution nearly equimolar of **11** and **12** showed a peak corresponding to the heterodimer (Figure 7).

The higher intensity peak for heterodimer over homodimers in **11–12** is evidence of formation of dimeric aggregates between the two pentakis-nucleosides corannulenes. However, neither the conformational details of the dimer nor intermolecular forces involved could be obtained from the MS data.

The ability of DNA corannulene derivative **18** to form ordered supramolecular assemblies was investigated by native PAGE and ssDNA-selective enzymatic digestion. Successful icosahedral supramolecular structure formation would require generation of complete annealing of 12 units of compound **18**, generating 30 dsDNA edges.

Two annealing strategies were pursued utilizing either kinetic control or thermodynamic control. In the kinetic strategy, a solution of **18** was first melted of any dsDNA at $95\text{ }^\circ\text{C}$, then was cooled to $4\text{ }^\circ\text{C}$ by immersion in an ice-bath. In the thermodynamic strategy, the melting step was followed by an annealing step at a temperature roughly $10\text{ }^\circ\text{C}$ below the

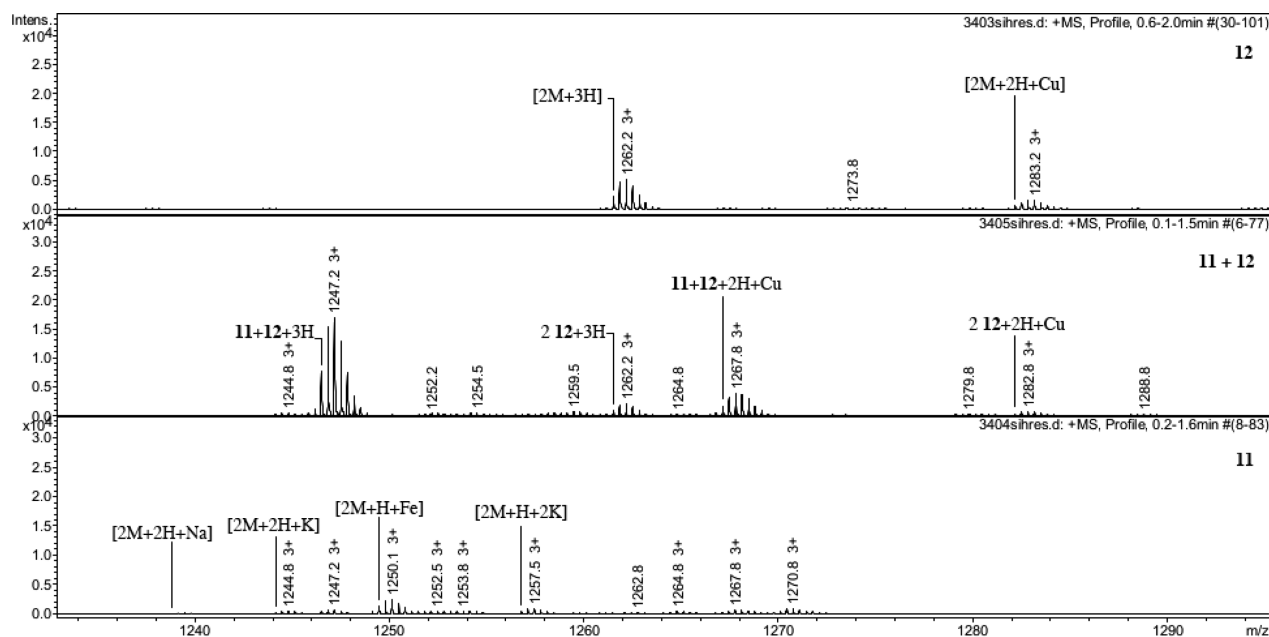


Figure 7. HR-ESI-MS in MeOH + 0.05% formic acid of **12** (top), mixture of **11** and **12** (middle), and **11** (bottom).

melting point of the double strand for at least an hour, and a final cooling step at 4 °C. Different outcomes were obtained from applying these two strategies to the same sample solution of **18** (1 μ M in TE Na⁺ 100 mM). Formation of small aggregates, mainly dimers and tetramers, was favored under thermodynamic control, whereas the kinetically controlled strategy achieved aggregates up to 12-mers. On the basis of this promising result, the annealing conditions were optimized, specifically the concentrations of **18**, Na⁺, and Mg²⁺ and time of the annealing step. The conditions maximizing formation of the 12-mer were found with the kinetically controlled protocol with a solution 2 μ M of **18** in TE buffer with Na⁺ 100 mM and Mg²⁺ 5 mM (Figure 8). By applying the thermodynamically controlled protocol, optimal conditions for dimer formation were achieved with a solution 1 μ M of **18** in TE buffer with Mg²⁺ 10 mM, and an annealing step of 50 h (Figure 8).

Mung bean nuclease (MBN)^{91,92} is an enzyme that selectively digests ssDNA, while not disturbing dsDNA. Therefore, in order to investigate the formation of the fully double-stranded dimer and 12-mer (icosahedral symmetric assembly), MBN digestion was carried out on the two annealed solutions of the dimer and 12-mer of **18** using the above protocols. The native PAGE of the samples shows all supramolecular aggregates to be digested by MBN, implying that neither the fully dsDNA strands associated with the dimer nor icosahedral supramolecular structures were formed.

Melting temperature (T_m) measurements were carried out on compound **18** to investigate stability of this annealed dimer system. Unfortunately, the temperature dependence of the absorption coefficient of corannulene at 260 nm did not permit accurate determination of T_m of the dsDNA formed under either kinetically or thermodynamically controlled conditions.

Computational Analysis. Due to its large size, the RM1 semiempirical Hamiltonian method was used to theoretically investigate the structural aspects of compound **18**, in particular, to investigate the potential for aggregation into cage-like supramolecular arrangements. The full theoretical model for the C₅-symmetric compound **18** is composed of 2875 atoms (8155 basis functions).

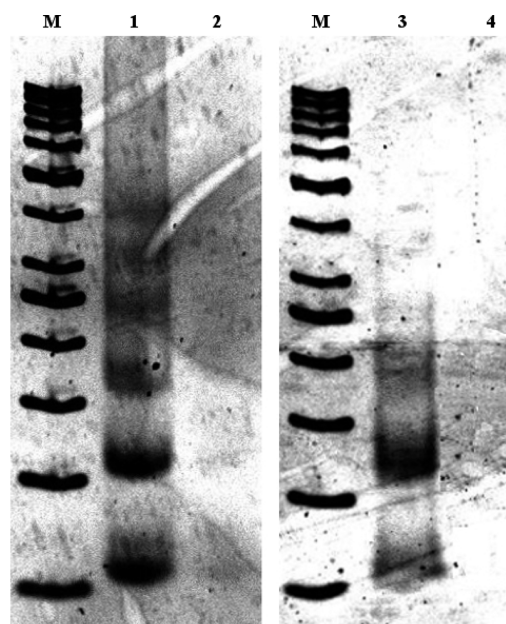


Figure 8. Native PAGE (4%) at 4 °C of assembling under kinetic (left) and thermodynamic control (right). Lanes M: 50 bp DNA ladder; lanes 1 and 3: assembled samples; lane 2 and 4: results from enzymatic digestion with MBN.

The RM1 optimized structure of the ssDNA-conjugated corannulene (Figure 9) is characterized by an arm-length of 75.1 Å, measuring from the center of corannulene to the oxygen of the final hydroxyl group of the ssDNA. The bowl depth, a characteristic geometric parameter associated with corannulene derivatives, was determined for corannulene in isolation at the RM1 level of theory to be 0.88 Å, comparing well to the experimentally observed bowl-depth, 0.87 Å.⁹³ The bowl depth for **18** is slightly more shallow than the isolated corannulene, at 0.85 Å, and therefore it is expected that this linker orientation would not be rigidly adopted, but interconvert as does corannulene.

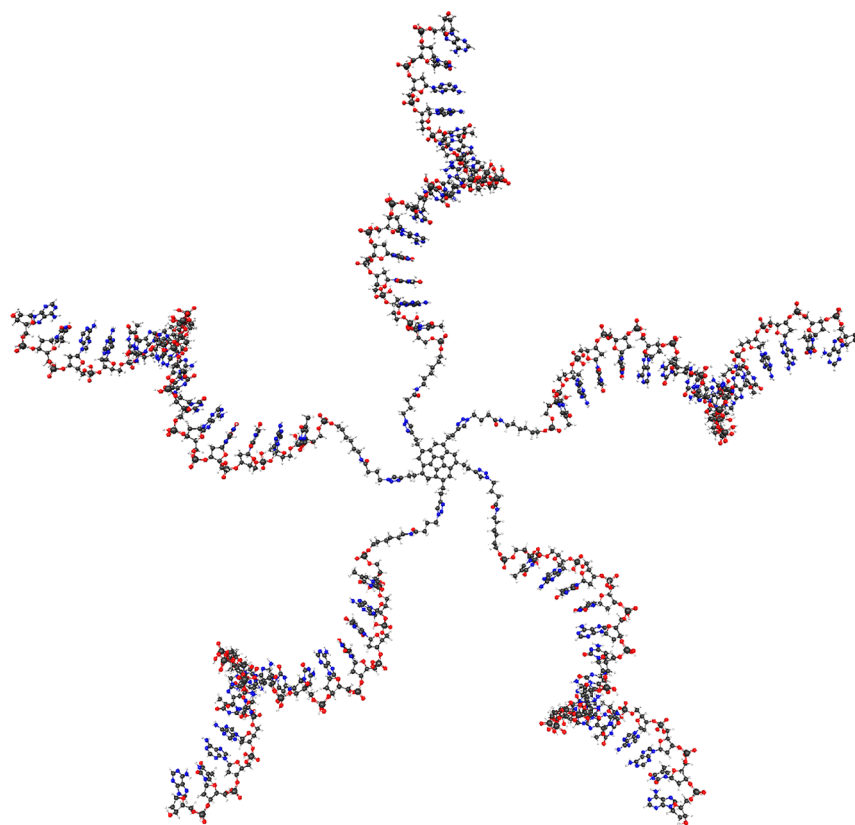


Figure 9. RM1 optimized ssDNA-conjugated corannulene.

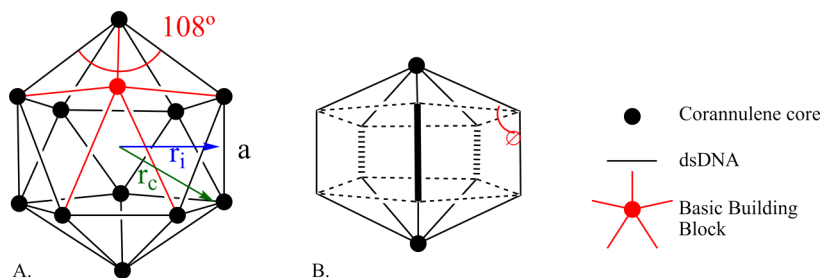


Figure 10. Supramolecular structures of **18** resulting from (A) 12-mer aggregation into an icosahedron or (B) dimer formation of a pentagonal prism.

The angle between neighboring arms measured from the center of corannulene is 71.9° , and 143.7° between non-neighboring arms. In an idealized icosahedron, these angles stemming from one vertex of a regular icosahedron are 60° and 108° , respectively, as illustrated in Figure 10, thus substantially smaller than observed in the optimized structure of **18**. This large discrepancy provides evidence for the lack of icosahedral 12-mer formation, and suggests implementation of a more rigid linker to the DNA to effectively restrict the angles of the bioconjugated arms closer to 108° , increasing the probability for icosahedron formation.

Annealing of the ssDNA arms enabled further investigation of how changes in arm length impact the side length of an icosahedral structure. RM1 geometry optimizations on the paired palindromic dsDNA strands were used to compare the length and associated interaction energies of the DNA strands. The binding energy for formation of dsDNA from two single ssDNA strands was determined as $E_{\text{binding}} = E_{\text{dsDNA}} - 2E_{\text{ssDNA}}$. Initially, the optimized dsDNA structure was separated into two

single ssDNA strands, and the energy of the fixed geometry determined, resulting in a binding energy of -244 kcal/mol. Relaxing the ssDNA geometry resulted in a 79 kcal/mol reduction in energy compared to the fixed geometry, enabling an estimation of the reorganization energy cost for bringing the ssDNA together into the dsDNA conformation. Including effects of reorganization, the final binding energy is determined to be -87 kcal/mol.

Comparison of the geometric features of ss- versus ds-DNA shows that the distance between the 3' and 5' ends of the relaxed ssDNA strand are shortened by only 1.3 Å in the dsDNA conformation. This results in a predicted icosahedral side length, a in Figure 10A, of 80.2 Å. Provided that the linkers assume a 108° angle within the constraints of a regular icosahedron, this would result in a supramolecular structure with inscribed sphere radius, $r_i = 60.6$ Å, and circumscribed sphere radius $r_c = 76.2$ Å.

In contrast to the icosahedral structure, a dimer structure could easily accommodate a more shallow corannulene-linker

structure, as calculated for **18**, but would necessitate the bending of the linker-to-DNA junction to an angle, θ in Figure 10, of 98° to properly orient the ssDNA strands for annealing. This angle in the calculated structure of **18** is a much more linear 165° , suggesting again a design modification to promote dimer formation, by rigidifying the linkers to DNA to achieve this orientation. With future optimization of the structure, formation of dimer supramolecular aggregate should be successful, especially considering the greater probability of two molecules joining in concert, opposed to association of 12 molecules in the correct orientation for icosahedral aggregation.

CONCLUSIONS

A powerful and robust procedure for the synthesis of fivefold symmetric pentasubstituted corannulene derivatives functionalized with the biomolecules (sugars, oligopeptide, nucleosides, and oligonucleotide) has been demonstrated. Studies characterizing aggregation behavior of these new constructs support formation of supramolecular architectures. Water-soluble galactoside derivatives of corannulene were observed to form H-dimers in solution, while dimeric structures can be formed between pentakis-nucleoside corannulene derivatives most probably via H-bonding. Particularly interesting and promising results for formation of corannulene-based supramolecular architectures were obtained with DNA functionalized pentapods. Unfortunately, the formation of fully double-stranded dimeric or icosahedral supramolecular structures was not achieved, potentially due to both thermodynamic and geometric factors. Icosahedral aggregates are highly symmetric structures, and therefore strongly entropically unfavorable, due to orientation-specific aggregation of 12 molecules in solution. Theoretical investigations of **18** predict a minimum energy structure with significant geometric deviations from those found in an icosahedral orientation. The fully double-stranded dimer is likely not formed due to sterics, and calculations also suggest that this molecular geometry is unsupportive of the annealing of all five dsDNA strands^{94,95} in a dimeric fashion.

Although formation of the icosahedral aggregate was not observed in this work, the predicted ~ 1.5 nm diameter nanocapsule offers interesting potential for applications given both the size and nature of its construction. This cavity size offers the capacity to enclose large cargo, such as small proteins or genes. The release of cargo could also be directed by the same parameters that affect the annealing of the DNA sequence, namely, temperature, ion and denaturant concentrations, and enzymatic activity. With ever-increasing applications for nanoscale delivery mechanisms in the fields of targeted medicine and materials science, DNA-based nanocapsules are an option of growing interest. Specifically, a bioconjugated-organic construct offers appealing advantages, including increased stability and rigidity of the organic framework, and potential for a longer lifetime in vivo due to lower degradation rates of organic compounds compared to purely biomolecular constructs. This work encourages the continuation of efforts toward the synthesis of bioconjugated-corannulene supramolecular structures, and together with ab initio structural analysis, improved design and success of organized dimer or 12-mer formation is expected.

EXPERIMENTAL SECTION

Synthetic procedures were carried out in an inert atmosphere of nitrogen, in dry solvents (by passage through alumina columns

in a MC Brown solvent system and degassed with N_2), using standard Schlenk techniques, unless otherwise noted. Oligopeptide H-Ala-Ala-Ala-OMe acetate salt was purchased from Bachem, 5'-modified oligonucleotide **19** was purchased from Metabion, mung bean nuclease was purchased from New England Biolabs, DNA ladder 50 bp was purchased from ThermoScientific, Float-A-Lyzer G2 was purchased from SpectrumLabs, and all the other reagents and solvents were purchased from Sigma Aldrich or VWR. All reagents and solvents were used without any further purification. Copper nanoparticles were prepared following a previously reported procedure.⁹⁶ Flash chromatographic purification was performed using silica gel Merck 60 (particle size 0.040–0.063 mm); the eluting solvent for each purification was determined by thin-layer chromatography (TLC). Analytical thin-layer chromatography was performed using Merck TLC silica gel 60 F254. Solvents for chromatography were technical grade and freshly distilled before use. Microwave reactions were carried out in a dedicated CEM Discovery microwave oven. The microwave power was limited by temperature control once the desired temperature was reached. 1H NMR spectra were recorded on a Bruker AV2–500 (500 MHz) spectrometer. Solvents for NMR spectroscopy were purchased from ARMAR chemicals, degassed with nitrogen, and dried over molecular sieves. Chemical shifts are reported in parts per million (ppm) relative to the solvent residual peaks: $CDCl_3 = 7.26$ ppm, d^4 -MeOD = 3.31 ppm, d^6 -DMSO = 2.50 ppm, and $D_2O = 4.79$ ppm. Multiplicities are given as s (singlet), br (broad), d (doublet), t (triplet), q (quadruplet), quint (quintet), m (multiplet). 1H -decoupled ^{13}C NMR spectra were obtained on a Bruker AV2–500 (125 MHz) spectrometer. ^{13}C NMR chemical shifts are reported relative to the solvent residual peaks: $CDCl_3 = 77.23$ ppm, d^4 -MeOD = 49.00 ppm, d^6 -DMSO = 39.52 ppm. UV/vis measurements were carried out on an Agilent 8453 UV/vis spectrophotometer using a 1 mm path quartz cuvette. Emission spectra were recorded on an Edinburgh Instruments FLS920 spectrometer with excitation at 300 nm. $[\alpha]_D$ values were recorded on JASCO P-2000 Polarimeter at $25^\circ C$. IR: Perkin-Elmer Spectrum One (FT-IR). HR-ESI-MS: Finnigan Mat 900 MS; MALDI-TOF-MS: Bruker Autoflex I using 3-HPA matrix. Circular dichroism spectra were recorded at room temperature on a Jasco J-810 spectropolarimeter using 1 mm path quartz cuvette. A Nanodrop 2000C was used for quantification of **18** in solution. AlphaImager from AlphaInnotech was used for visualization of gels stained with ethidium bromide.

sym-Penta-2-(1,2,3-triazole-1-(2,3,5-tri-O-acetyl- β -ribofuranosyl)-4-ethyl)-corannulene (7). A mixture of *sym*-penta-(1-butyn-4-yl)-corannulene **3**⁵⁸ (10.0 mg, 20 μ mol), 2,3,5-tri-O-acetyl- β -D-ribofuranosyl-1-azide **6**⁶² (62.0 mg, 21 mmol) and copper nanoparticles (13.2 mg, 0.21 mmol) in DMF (1.0 mL) in a microwave vessel was heated at $80^\circ C$ in a microwave reactor (200 W) for 8 h. The mixture was then filtrated over Celite and the solvent was evaporated. The product was purified by column chromatography on silica gel eluted with a solution of DCM:MeOH 96:4. The solvent was evaporated to yield a yellow solid (21.6 mg, 54%). 1H NMR (500 MHz, $CDCl_3$): δ 7.62 (s, 5H), 7.55 (s, 5H), 6.11 (d, $J = 3.5$ Hz, 5H), 5.81 (t, $J = 4.0$ Hz, 5H), 5.60 (t, $J = 5.0$ Hz, 5H), 4.42 (m, 5H), 4.32 (dd, $J = 12.5, 3.5$ Hz, 5H), 4.19 (dd, $J = 12.5, 4.5$ Hz, 5H), 3.50 (m, 10H), 3.29 (m, 10H), 2.10 (s, 15H), 2.08 (s, 15H), 1.97 (s, 15H). ^{13}C NMR (125 MHz, $CDCl_3$): δ 170.5, 169.5, 169.4, 147.7, 140.3, 135.1, 129.7, 123.1, 120.9, 90.0, 80.9, 74.4, 71.0, 63.1, 33.1, 29.8, 28.3, 20.8, 20.6,

20.5. IR (KBr): ν cm^{-1} 3422, 2927, 2854, 1750, 1445, 1437, 1373, 1231, 1091, 1062, 1041, 923, 900, 811, 730, 602. UV (DMSO) λ_{max} nm: 264, 299. $[\alpha]_{\text{D}} = -17.4$ ($c = 0.008$ in DMSO). HRMS (ESI) m/z : found 1030.8341 ($M + 2\text{Na}$); calc ($\text{C}_{95}\text{H}_{105}\text{N}_{15}\text{Na}_2\text{O}_{35}$) 1030.8341.

sym-Penta-2-(1,2,3-triazole-1-(- β -ribofuranosyl)-4-ethyl)-corannulene (5). A solution of 7 (9.2 mg, 4.6 μmol) and MeONa (16.5 mg, 0.31 mmol) in MeOH (1.5 mL) was stirred under nitrogen at room temperature for 2 days. Dowex 50 was added until pH 6 was reached. The mixture was filtrated and the solvent was evaporated. The product is a yellow solid (6.0 mg, 94%). ^1H NMR (500 MHz, d^6 -DMSO): δ 8.25 (s, 5H), 7.86 (s, 5H), 5.91 (d, $J = 4.5$ Hz, 5H), 5.63 (d, $J = 5.5$ Hz, 5H), 5.30 (d, $J = 3.5$ Hz, 5H), 4.99 (t, $J = 5.0$ Hz, 5H), 4.36 (d, $J = 4.5$ Hz, 5H), 4.11 (d, $J = 3.5$ Hz, 5H), 3.95 (q, $J = 4.5$ Hz, 5H), 3.61 – 3.48 (m, 20H), 3.21 (br, 10H). ^{13}C NMR (125 MHz, d^6 -DMSO): δ 146.7, 140.6, 134.1, 129.5, 123.0, 120.8, 109.5, 92.0, 85.7, 75.1, 70.4, 61.4, 32.4, 28.0. IR (KBr): ν cm^{-1} 3359, 2924, 2853, 1595, 1454, 1383, 1331, 1228, 1101, 1047, 863, 824, 755, 102, 621. UV (DMSO) λ_{max} nm: 264, 300. $[\alpha]_{\text{D}} = +255.0$ ($c = 0.004$ in DMSO). HRMS (ESI) m/z : found 1408.5211 ($M + \text{Na}$); calc ($\text{C}_{65}\text{H}_{75}\text{N}_{15}\text{NaO}_{20}$) 1408.5205.

N-(2-Azide-propionyl)-di-L-alanine Methyl Ester (10). Triflic anhydride (0.65 mL, 3.88 mmol) was added to a solution of NaN_3 (1.2 g, 18.5 mmol) in DCM (3.0 mL) and water (2.0 mL) at 0 °C; the reaction was stirred at room temperature for 2 h. The organic phase was separated and the aqueous extracted with DCM. The reunited organic phases were washed with a saturated solution of NaHCO_3 . The organic phase was then added to a solution of H-Ala-Ala-Ala-OMe acetate salt (454 mg, 1.49 mmol), $\text{CuSO}_4 \cdot 5\text{H}_2\text{O}$ (5.6 mg, 0.02 mmol) and K_2CO_3 (387 mg, 2.80 mmol) in methanol (6.6 mL) and water (3.2 mL) at room temperature; the mixture was stirred for 22 h. The organic layer was then separated and the aqueous phase was extracted with DCM. The reunited organic phases were dried over Na_2SO_4 and evaporated to yield the crude product. The product was purified by column chromatography on silica gel eluted with a mixture DCM:MeOH 9:1. The solvent was evaporated to yield a white solid (211 mg, 52%). ^1H NMR (500 MHz, CDCl_3): δ 6.89 (d, $J = 6.5$ Hz, 1H), 6.43 (d, $J = 6.5$ Hz, 1H), 4.56 (quint, $J = 7.0$ Hz, 1H), 4.42 (quint, $J = 7.0$ Hz, 1H), 4.07 (q, $J = 7.0$ Hz, 1H), 3.76 (s, 3H), 1.53 (d, $J = 7.0$ Hz, 3H), 1.42 (d, $J = 7.0$ Hz, 3H), 1.41 (d, $J = 7.0$ Hz, 3H). ^{13}C NMR (125 MHz, CDCl_3): δ 173.2, 171.3, 169.8, 59.1, 52.7, 48.9, 48.4, 18.5, 18.4, 17.2. IR (KBr): ν cm^{-1} 3312, 2972, 2116, 2078, 1740, 1641, 1546, 1450, 1376, 1344, 1325, 1218, 1162, 1106, 1073, 1063, 1008, 984, 956, 855, 663, 572. $[\alpha]_{\text{D}} = -104.7$ ($c = 0.0040$ in CHCl_3). HRMS (ESI) m/z : found 294.1174 ($M + \text{Na}$); calc ($\text{C}_{10}\text{H}_{17}\text{N}_3\text{NaO}_4$) 294.1173.

sym-Penta-2-(1,2,3-triazole-1-(N-(2-methyl-acetyl)-di-L-alanine methyl ester)-4-ethyl)-corannulene (9). A mixture of *sym*-penta-(1-butyn-4-yl)-corannulene **3**⁵⁸ (9.1 mg, 18 μmol), *N*-(2-azide-propionyl)-di-L-alanine methyl ester **10** (50.3 mg, 0.19 mmol), and copper nanoparticles (13.4 mg, 0.21 mmol) in DMF (0.5 mL) in a microwave vessel was heated at 80 °C in a microwave reactor (200 W) for 8 h. The mixture was then filtrated over Celite and the solvent was evaporated. The product was purified by column chromatography on silica gel eluted with a DCM:MeOH 9:1. The solvent was evaporated to yield a yellow solid (19 mg, 57%). ^1H NMR (500 MHz, d^6 -DMSO): δ 8.60 (d, $J = 7.5$ Hz, 5H), 8.39 (d, $J = 7.0$ Hz, 5H), 8.09 (s, 5H), 7.82 (s, 5H), 5.43 (q, $J = 7.0$ Hz, 5H), 4.27 (m, 10H), 3.61 (s, 15H), 3.47 (br, 10H), 3.18 (br, 10H), 1.60 (d, J

= 7.0 Hz, 15H), 1.27 (d, $J = 7.5$ Hz, 15H), 1.21 (d, $J = 7.0$ Hz, 15H). ^{13}C NMR (125 MHz, d^6 -DMSO): δ 173.0, 171.8, 168.4, 146.0, 140.6, 134.1, 129.5, 123.0, 121.4, 57.7, 51.9, 48.0, 47.5, 32.5, 28.1, 18.2, 18.1, 16.8. IR (KBr): ν cm^{-1} 3290, 2930, 1741, 1645, 1551, 1455, 1383, 1329, 1222, 1164, 1052, 998, 953, 684. UV (DMSO) λ_{max} nm: 264, 299. $[\alpha]_{\text{D}} = +3.7$ ($c = 0.055$ in DMSO). HRMS (ESI) m/z : found 955.9273 ($M + 2\text{Na}$); calc ($\text{C}_{90}\text{H}_{115}\text{N}_{25}\text{Na}_2\text{O}_{20}$) 955.9267.

5'-Azido-2',5'-dideoxy-adenosine (15). A solution of 5'-*O*-toluenesulphonyl-2'-deoxy-adenosine **14**⁶⁵ (270 mg, 6.67 mmol) in dry DMF (2.0 mL) was added dropwise to a mixture of LiN_3 (525 mg, 10.7 mmol) in dry DMF (1.0 mL). The reaction mixture was stirred at room temperature for 2 days; the solvent was evaporated and the product was purified by column chromatography on silica gel eluted with a DCM:MeOH:TEA 9:1:0.25. The solvent was evaporated to yield a colorless foam (140 mg, 76%). The spectroscopic data were identical with those reported.⁹⁷ ^1H NMR (500 MHz, d^4 -MeOD): δ 8.29 (s, 1H), 8.21 (s, 1H), 6.44 (t, $J = 7.0$ Hz, 1H), 4.57 (m, 1H), 4.08 (m, 1H), 3.64 (dd, $J = 13.5$, 6.0 Hz, 1H), 3.56 (dd, $J = 13.5$, 4.0 Hz, 1H), 2.96 (m, 1H), 2.49 (m, 1H). ^{13}C NMR (125 MHz, d^4 -MeOD): δ 154.0, 141.3, 130.0, 127.1, 87.3, 85.9, 73.0, 53.5, 47.5, 40.4.

sym-Penta-2-(1,2,3-triazole-1-(5'-yl-2',5'-dideoxy-adenosine)-4-ethyl)-corannulene (12). A mixture of *sym*-penta-(1-butyn-4-yl)-corannulene **3**⁵⁸ (10 mg, 19.6 μmol), 5'-azido-2',5'-dideoxy-adenosine **15** (65.1 mg, 0.24 mmol) and copper nanoparticles (10.1 mg, 0.16 mmol) in DMF (1.0 mL) in a microwave vessel was heated at 60 °C in a microwave reactor (200 W) for 2 h. The mixture was then filtrated over Celite and the solvent was evaporated and MeOH was added to the crude. The solid was then filtrated, washed with cold MeOH, and recrystallized from water to yield a reddish solid (14.5 mg, 40%). ^1H NMR (500 MHz, d^6 -DMSO, 373 K): δ 8.18–8.16 (m, 10H), 7.75 (s, 5H), 7.71 (s, 5H), 6.91 (br s, 10H), 6.35 (t, $J = 6.5$ Hz, 5H), 5.31 (d, $J = 5.0$ Hz, 5H), 4.70 (dd, $J = 14.0$, 4.5 Hz, 5H), 4.61 (dd, $J = 14.5$, 7.0 Hz, 5H), 4.53 (br s, 5H), 4.23 (br s, 5H), 3.42 (t, $J = 7.0$ Hz, 10H), 3.14 (t, $J = 7.5$ Hz, 10H), 2.80 (m, 5H), 2.36 (m, 5H). ^{13}C NMR (125 MHz, d^6 -DMSO): δ 156.1, 152.6, 149.2, 146.3, 140.4, 139.8, 133.9, 129.4, 128.0, 125.5, 122.8, 84.9, 83.6, 71.1, 67.0, 64.9, 51.4, 38.1, 32.3, 27.7, 25.1. IR (KBr): ν cm^{-1} 3329, 3186, 2928, 1653, 1647, 1640, 1599, 1577, 1474, 1420, 1366, 1331, 1299, 1248, 1217, 1087, 1056, 939, 797, 726, 649. UV (DMSO) λ_{max} nm: 265, 299. $[\alpha]_{\text{D}} = +25.6$ ($c = 0.008$ in DMSO). HRMS (ESI) m/z : found 946.3962 ($M + 2\text{H}$); calc ($\text{C}_{90}\text{H}_{92}\text{N}_{40}\text{O}_{10}$) 946.3955.

sym-Penta-2-(1,2,3-triazole-1-(5'-yl-2'-deoxy-ribo-thymidine)-4-ethyl)-corannulene (11). A mixture of *sym*-penta-(1-butyn-4-yl)-corannulene **3**⁵⁸ (9.9 mg, 19.4 μmol), 5'-azido thymidine **17**⁶⁶ (43.0 mg, 0.16 mmol), and copper nanoparticles (10.9 mg, 0.17 mmol) in DMF (1.0 mL) in a microwave vessel was heated at 60 °C in a microwave reactor (200 W) for 2 h. The mixture was then filtrated over Celite and the solvent was evaporated and MeOH was added to the crude. The solid was then filtrated and washed with cold MeOH to yield a pale yellow solid (24.6 mg, 69%). ^1H NMR (500 MHz, d^6 -DMSO): δ 11.30 (s, 5H), 7.98 (s, 5H), 7.77 (s, 5H), 7.31 (s, 5H), 6.15 (t, $J = 6.5$ Hz, 5H), 5.49 (d, $J = 4.5$ Hz, 5H), 4.69–4.58 (m, 10H), 4.27 (m, 5H), 4.06 (m, 5H), 3.45 (br, 10H), 3.17 (d, $J = 5.0$ Hz, 10H), 2.15–2.07 (m, 10H), 1.75 (s, 15H). ^{13}C NMR (125 MHz, d^6 -DMSO): δ 163.7, 150.4, 146.4, 140.4, 136.1, 134.1, 129.4, 123.1, 109.8, 84.1, 84.0, 70.7, 51.1, 48.6,

37.9, 32.4, 27.9, 12.1. IR (KBr): ν cm⁻¹ 3421, 2926, 1688, 1472, 1438, 1273, 1221, 1135, 1084, 1056, 958, 874, 766, 558. UV (DMSO) λ_{max} nm: 265, 298. $[\alpha]_{\text{D}} = +108.5$ ($c = 0.012$ in DMSO). HRMS (ESI) m/z : found 923.8662 ($M + 2H$); calc ($C_{90}H_{97}N_{25}O_{20}$) 923.8665.

Pentakis-DNA Corannulene (18). Ten μL of a solution of CuBr (92 μg , 0.64 μmol) and TBTA (0.546 mg, 1.0 μmol) in water:THF 1:1 (100 μL) was added to a solution of *sym*-penta-(1-butyn-4-yl)-corannulene **3**⁵⁸ (49 μg , 96 nmol) and oligonucleotide **19** (1.1 μmol) in THF (5 μL) and water (15 μL) and heated at 60 °C for 2 days and at 80 °C for 4 days. The reaction mixture was then desalted with Sephadex G-25. The crude product was then purified by 6% D-PAGE (acrylamide:bisacrylamide 19:1, Urea 7 M) at constant power of 40 W, using TBE buffer (Tris 11 g, boric acid 5.6 g, and EDTA 0.74 g in 1 L of sterile water). Following electrophoresis, the plate was wrapped in plastic and placed on a fluorescent TLC plate and illuminated with UV lamp (254 nm). The band was quickly excised, and the gel pieces were frozen with liquid nitrogen, crushed, and incubated overnight in 2 volumes of NaOAc (0.5 M, pH 5.2 with HCl) at 37 °C. The samples were then centrifuged and the supernatant collected. The gel was then washed with 1/5 volume of NaOAc 0.5 M, centrifuged, and the supernatant collected. The aqueous solution was then extracted with *n*-butanol to 1/3 of the original volume. 0.16 volume of a solution of LiCl 4 M and MgCl₂ 0.125 mM and 3 volumes of cold ethanol (100%, -80 °C) were added to the aqueous solution and stored overnight at -80 °C. The sample was then centrifuged (13200 rpm, 4 °C, 20 min) and the supernatant was removed. The precipitate was washed 3 times with cold ethanol (80%, 0 °C), dissolved in sterile Milli-Q water and desalted with Float-A-Lyzer G2. The amount of **18** was quantified by UV absorption (300 nm assuming $\epsilon = 3.28 \times 10^4$). The sample was then freeze-dried yielding the desired product as a pale yellow powder (304 μg , 12%). MALDI-TOF MS m/z found 26483.2 ($M + 5\text{Na} + 18\text{H}$); calc. ($C_{875}H_{1195}N_{315}O_{490}P_{80}Na_2Li$) 26483.7241.

Assembling Studies. Kinetically Controlled Procedure. A 2 μM solution of **18** in TE buffer (Tris 10 mM, EDTA 1 mM pH 7.5 with HCl) with NaCl 100 mM and MgCl₂ 5 mM was heated for 5 min at 95 °C in a heating block; the sample was then transferred in an ice-bath, kept at 0 °C for 10 min and then loaded on the gel.

Thermodynamically Controlled Procedure. A 1 μM solution of **18** in TE buffer (Tris 10 mM, EDTA 1 mM pH 7.5 with HCl) with MgCl₂ 10 mM was heated for 5 min at 95 °C in a heating block, then slowly cooled to 55 °C, kept at this temperature for 50 h, then slowly cooled to 4 °C and loaded on the gel.

Native PAGE. The samples from assembling studies were analyzed by 4% native-PAGE (acrylamide:bisacrylamide 19:1) at 4 °C and at constant current of 10 mA for 1.5 h. The gels were stained with ethidium bromide.

Enzymatic Digestion. Digestion of single-stranded DNA with mung bean nuclease was performed for 3 h at 0 °C in sodium acetate buffer (10 mM, Zn(OAc)₂ 0.1 mM, cysteine 1 mM, Triton X-100 0.001%, and glycerol 50%) applying 10 units of mung bean nuclease per μg of **18**.

Computational Methodology. The long-standing widespread application of the AM1 and the PM-series SE methods attest to the utility and reliability of these low-cost ab initio options. Recently, the relatively new RM1 semiempirical Hamiltonian method was implemented into the computational

chemistry package, GAMESS.⁹⁸ The RM1 method, developed by Rocha GB et al.,⁹⁹ has the ten most common elements for bioorganic systems, H, C, N, O, F, P, S, Cl, Br, and I, fully optimized using a training set of 1736 molecules representative of organic and biochemical systems. This reparameterization has been demonstrated to achieve greater accuracy in calculations of enthalpies of formation, dipole moments, ionization potentials, and interatomic distances, on biosystems, in comparison to other available semiempirical Hamiltonians. Full geometry optimization was carried out for the DNA-conjugated corannulene system **18**, as well as several other components described. Optimization was carried out in gas phase, and therefore the charge of the DNA backbone was neutralized by the addition of hydrogen atoms to each phosphate group. For the purposes of this investigation, effects of solution environment are not expected to significantly change the conclusions of the theoretical analysis.

■ ASSOCIATED CONTENT

Supporting Information

¹H NMR, ¹³C NMR, FTIR, and MS spectra for all the pertinent compounds and MBN digestion test on dsDNA. This material is available free of charge via the Internet at <http://pubs.acs.org>.

■ AUTHOR INFORMATION

Corresponding Authors

*Tel: +41 44 635 4201; E-mail: kimb@oci.uzh.ch.

*Tel: +86-22-87402050; E-mail: dean_spst@tju.edu.cn.

Notes

The authors declare no competing financial interest.

■ ACKNOWLEDGMENTS

We gratefully acknowledge the Swiss National Science Foundation for support of this work. We are grateful to the NMR and MS facilities at UZH (O. Zerbe and L. Bigler). We thank U. Rieder, S. Gallo, J. Marino, and O. Schmidt for the help and useful discussion. J.S.S. thanks the Synergetic Innovation Center of Chemical Science and Engineering (Tianjin University, Tianjin, China).

■ REFERENCES

- (1) Sharma, J., Chhabra, R., Cheng, A., Brownell, J., Liu, Y., and Yan, H. (2009) Control of self-assembly of DNA tubules through integration of gold nanoparticles. *Science* 323, 112–116.
- (2) Furukawa, H., and Yaghi, O. M. (2009) Storage of hydrogen, methane, and carbon dioxide in highly porous covalent organic frameworks for clean energy applications. *J. Am. Chem. Soc.* 131, 8875–8883.
- (3) Scheinberg, D. A., Villa, C. H., Escorcía, F. E., and McDevitt, M. R. (2010) Conscripts of the infinite armada: systemic cancer therapy using nanomaterials. *Nat. Rev. Clin. Oncol.* 7, 266–276.
- (4) Vance, D., Martin, J., Patke, S., and Kane, R. S. (2009) The design of polyvalent scaffolds for targeted delivery. *Adv. Drug Delivery Rev.* 61, 931–939.
- (5) Scharnagl, N., Lee, S., Hiebl, B., Sisson, A., and Lendlein, A. (2010) Design principles for polymers as substratum for adherent cells. *J. Mater. Chem.* 20, 8789–8802.
- (6) Ajami, D., and Rebek, J. (2009) Compressed alkanes in reversible encapsulation complexes. *Nat. Chem.* 1, 87–90.
- (7) Brown, C. J., Bergman, R. G., and Raymond, K. N. (2009) Enantioselective catalysis of the aza-cope rearrangement by a chiral supramolecular assembly. *J. Am. Chem. Soc.* 131, 17530–17531.

- (8) Murase, T., Horiuchi, S., and Fujita, M. (2010) Naphthalene diels-alder in a self-assembled molecular flask. *J. Am. Chem. Soc.* 132, 2866–2867.
- (9) Clark, T. D., Kobayashi, K., and Ghadiri, M. R. (1999) Covalent capture and stabilization of cylindrical β -sheet peptide assemblies. *Chem.—Eur. J.* 5, 782–792.
- (10) Lehn, J.-M. (1995) *Supramolecular chemistry*; Wiley-VCH Verlag GmbH & Co. KGaA: Weinheim.
- (11) Hartgerink, J. D., Clark, T. D., and Ghadiri, M. R. (1998) Peptide nanotubes and beyond. *Chem.—Eur. J.* 4, 1367–1372.
- (12) Vögtle, F. (1996) *Comprehensive supramolecular chemistry*; Pergamon: Oxford.
- (13) Ghadiri, M. R., Granja, J. R., Milligan, R. A., McRee, D. E., and Khazanovich, N. (1993) Self-assembling organic nanotubes based on a cyclic peptide architecture. *Nature* 366, 324–327.
- (14) Brunsveld, L., Folmer, B. J. B., and Meijer, E. W. (2000) Supramolecular polymers. *MRS Bull.* 25, 49–53.
- (15) Meijer, E. W., Ky Hirschberg, J. H. K., Brunsveld, L., Ramzi, A., Vekemans, J. A. J. M., and Sijbesma, R. P. (2000) Helical self-assembled polymers from cooperative stacking of hydrogen-bonded pairs. *Nature* 407, 167–170.
- (16) Engelkamp, H. (1999) Self-assembly of disk-shaped molecules to coiled-coil aggregates with tunable helicity. *Science* 284, 785–788.
- (17) Isaacs, L., Chin, D. N., Bowden, X., Xia, Y., and Whitesides, G. M. (1999) Self-assembling systems on scales from nanometers to millimeters: design and discovery. *Perspect. Supramol. Chem.* 4, 1–46.
- (18) Whitesides, G., Mathias, J., and Seto, C. (1991) Molecular self-assembly and nanochemistry: a chemical strategy for the synthesis of nanostructures. *Science* 254, 1312–1319.
- (19) MacDonald, J. C., and Whitesides, G. M. (1994) Solid-state structures of hydrogen-bonded tapes based on cyclic secondary diamides. *Chem. Rev.* 94, 2383–2420.
- (20) Hudson, S. D. (1997) Direct visualization of individual cylindrical and spherical supramolecular dendrimers. *Science* 278, 449–452.
- (21) Percec, V., Ahn, C.-H., Ungar, G., Yeardley, D. J. P., Möller, M., and Sheiko, S. S. (1998) Controlling polymer shape through the self-assembly of dendritic side-groups. *Nature* 391, 161–164.
- (22) Zimmerman, S. C., Zeng, F., Reichert, D. E. C., and Kolotuchin, S. V. (1996) Self-assembling dendrimers. *Science* 271, 1095–1098.
- (23) Hartgerink, J. D. (2001) Self-assembly and mineralization of peptide-amphiphile nanofibers. *Science* 294, 1684–1688.
- (24) Hartgerink, J. D. (2002) Supramolecular chemistry and self-assembly special feature: peptide-amphiphile nanofibers: a versatile scaffold for the preparation of self-assembling materials. *Proc. Natl. Acad. Sci. U.S.A.* 99, 5133–5138.
- (25) Claussen, R. C., Rabatic, B. M., and Stupp, S. I. (2003) Aqueous self-assembly of unsymmetric peptide bolaamphiphiles into nanofibers with hydrophilic cores and surfaces. *J. Am. Chem. Soc.* 125, 12680–12681.
- (26) Tsai, W.-W., Li, L.-s., Cui, H., Jiang, H., and Stupp, S. I. (2008) Self-assembly of amphiphiles with terthiophene and tripeptide segments into helical nanostructures. *Tetrahedron* 64, 8504–8514.
- (27) Cui, H., Muraoka, T., Cheetham, A. G., and Stupp, S. I. (2009) Self-assembly of giant peptide nanobelts. *Nano Lett.* 9, 945–951.
- (28) Pashuck, E. T., Cui, H., and Stupp, S. I. (2010) Tuning supramolecular rigidity of peptide fibers through molecular structure. *J. Am. Chem. Soc.* 132, 6041–6046.
- (29) Schneider, J., Cui, H., Webber, M. J., and Stupp, S. I. (2010) Self-assembly of peptide amphiphiles: from molecules to nanostructures to biomaterials. *Biopolymers* 94, 1–18.
- (30) Gissot, A., Camplo, M., Grinstaff, M. W., and Barthélémy, P. (2008) Nucleoside, nucleotide and oligonucleotide based amphiphiles: a successful marriage of nucleic acids with lipids. *Org. Biomol. Chem.* 6, 1324–1333.
- (31) Nowick, J. S., Cao, T., and Noronha, G. (1994) Molecular recognition between uncharged molecules in aqueous micelles. *J. Am. Chem. Soc.* 116, 3285–3289.
- (32) Li, C., Huang, J., and Liang, Y. (2000) Molecular recognition capabilities of a nucleolipid amphiphile (3',5'-distearoyl)-2'-deoxythymidine to adenosine at the air/water interface and Langmuir-Blodgett films studied by molecular spectroscopy. *Langmuir* 16, 7701–7707.
- (33) Berndt, P., Kurihara, K., and Kunitake, T. (1995) Measurement of forces between surfaces composed of two-dimensionally organized, complementary and noncomplementary nucleobases. *Langmuir* 11, 3083–3091.
- (34) Kim, B.-S., Hong, D.-J., Bae, J., and Lee, M. (2005) Controlled self-assembly of carbohydrate conjugate rod-coil amphiphiles for supramolecular multivalent ligands. *J. Am. Chem. Soc.* 127, 16333–16337.
- (35) Dal Bó, A. G., Soldi, V., Giacomelli, F. C., Travelet, C., Jean, B., Pignot-Paintrand, I., Borsali, R., and Fort, S. (2012) Self-assembly of amphiphilic glycoconjugates into lectin-adhesive nanoparticles. *Langmuir* 28, 1418–1426.
- (36) Yang, J. S., Zhou, Q. Q., and He, W. (2013) Amphipathicity and self-assembly behavior of amphiphilic alginate esters. *Carbohydr. Polym.* 92, 223–227.
- (37) Seeman, N. C. (1982) Nucleic acid junctions and lattices. *J. Theor. Biol.* 99, 237–247.
- (38) Chen, J., and Seeman, N. C. (1991) Synthesis from DNA of a molecule with the connectivity of a cube. *Nature* 350, 631–633.
- (39) Zhang, Y., and Seeman, N. C. (1994) Construction of a DNA-truncated octahedron. *J. Am. Chem. Soc.* 116, 1661–1669.
- (40) Seeman, N. C. (1998) Nucleic acid nanostructures and topology. *Angew. Chem., Int. Ed.* 37, 3220–3238.
- (41) Olson, A. J., Hu, Y. H. E., and Keinan, E. (2007) Chemical mimicry of viral capsid self-assembly. *Proc. Natl. Acad. Sci. U.S.A.* 104, 20731–20736.
- (42) Alvarez, S. (2005) Polyhedra in (inorganic) chemistry. *Dalton Trans.*, 2209–2233.
- (43) McKinlay, R. M., Dalgarno, S. J., Nichols, P. J., Papadopoulos, S., Atwood, J. L., and Raston, C. L. (2007) Icosahedral galloxxane clusters. *Chem. Commun.*, 2393–2395.
- (44) Müller, A., Sarkar, S., Shah, S. Q. N., Bögge, H., Schmidtman, M., Sarkar, S., Kögerler, P., Hauptfleisch, B., Trautwein, A. X., and Schünemann, V. (1999) Archimedean synthesis and magic numbers: “sizing” giant molybdenum-oxide-based molecular spheres of the keplerate type. *Angew. Chem., Int. Ed.* 38, 3238–3241.
- (45) Baldrige, K. K., and Siegel, J. S. (1997) Corannulene-based fullerene fragments $C_{20}H_{10}$ - $C_{50}H_{10}$. *Theor. Chem. Acc.* 97, 67–71.
- (46) Wu, Y.-T., Hayama, T., Baldrige, K. K., Linden, A., and Siegel, J. S. (2006) Synthesis of fluoranthenes and indenocorannulenes: elucidation of chiral stereoisomers on the basis of static molecular bowls. *J. Am. Chem. Soc.* 128, 6870–6884.
- (47) Sygula, A., Folsom, H. E., Sygula, R., Abdourazak, A. H., Marcinow, Z., Fronczek, F. R., and Rabideau, P. W. (1994) Bowl stacking in curved polynuclear aromatic hydrocarbons: crystal and molecular structure of cyclopentacorannulene. *J. Chem. Soc., Chem. Commun.*, 2571–2572.
- (48) Wu, Y.-T., Bandera, D., Maag, R., Linden, A., Baldrige, K. K., and Siegel, J. S. (2008) Multiethynyl corannulenes: synthesis, structure, and properties. *J. Am. Chem. Soc.* 130, 10729–10739.
- (49) Schmidt, B. M., Seki, S., Topolinski, B., Ohkubo, K., Fukuzumi, S., Sakurai, H., and Lentz, D. (2012) Electronic properties of trifluoromethylated corannulenes. *Angew. Chem., Int. Ed.* 51, 11385–11388.
- (50) Kuvychko, I. V., Spisak, S. N., Chen, Y.-S., Popov, A. A., Petrukina, M. A., Strauss, S. H., and Boltalina, O. V. (2012) A buckyball with a lot of potential C_5 - $C_{20}H_5(CF_3)_5$. *Angew. Chem., Int. Ed.* 51, 4939–4942.
- (51) Miyajima, D., Tashiro, K., Araoka, F., Takezoe, H., Kim, J., Kato, K., Takata, M., and Aida, T. (2009) Liquid crystalline corannulene responsive to electric field. *J. Am. Chem. Soc.* 131, 44–45.
- (52) Blinov, L. M. (1998) On the way to polar achiral liquid crystals. *Liq. Cryst.* 24, 143–152.

- (53) Atwood, J. L., Barbour, L. J., Hardie, M. J., and Raston, C. L. (2001) Metal sulfonatocalix[4,5]arene complexes: bi-layers, capsules, spheres, tubular arrays and beyond. *Coord. Chem. Rev.* 222, 3–32.
- (54) Xu, B., and Swager, T. M. (1993) Rigid bowlic liquid crystals based on tungsten-oxo calix[4]arenes: host-guest effects and head-to-tail organization. *J. Am. Chem. Soc.* 115, 1159–1160.
- (55) Miyajima, D., Araoka, F., Takezoe, H., Kim, J., Kato, K., Takata, M., and Aida, T. (2012) Ferroelectric columnar liquid crystal featuring confined polar groups within core-shell architecture. *Science* 336, 209–213.
- (56) Butterfield, A. M., Gilomen, B., and Siegel, J. S. (2012) Kilogram-scale production of corannulene. *Org. Process Res. Dev.* 16, 664–676.
- (57) Grube, G. H., Elliott, E. L., Steffens, R. J., Jones, C. S., Baldrige, K. K., and Siegel, J. S. (2003) Synthesis and properties of *sym*-pentasubstituted derivatives of corannulene. *Org. Lett.* 5, 713–716.
- (58) Mattarella, M., and Siegel, J. S. (2012) *Sym*-(CH₂X)₅-corannulenes: molecular pentapods displaying functional group and bioconjugate appendages. *Org. Biomol. Chem.* 10, 5799–5802.
- (59) Mattarella, M., Haberl, J., Ruokolainen, J., Landau, E. M., Mezzenga, R., and Siegel, J. S. (2013) Five-fold symmetric pentasubstituted corannulene with gelation properties and liquid crystalline phase. *Chem. Commun.* 49, 7204–7206.
- (60) Mattarella, M., Garcia-Hartjes, J., Wennekes, T., Zuilhof, H., and Siegel, J. S. (2013) Nanomolar cholera toxin inhibitors based on symmetrical pentavalent ganglioside GM1os-*sym*-corannulenes. *Org. Biomol. Chem.* 11, 4333–4339.
- (61) Chabre, Y. M., and Roy, R. (2013) Multivalent glycoconjugate syntheses and applications using aromatic scaffolds. *Chem. Soc. Rev.* 42, 4657–4708.
- (62) Hou, S., Liu, W., Ji, D., and Zhao, Z. (2011) Efficient synthesis of triazole moiety-containing nucleotide analogs and their inhibitory effects on a malic enzyme. *Bioorg. Med. Chem. Lett.* 21, 1667–1669.
- (63) Klok, H.-A., Rösler, A., Gütz, G., Mena-Osteritz, E., and Bäuerle, P. (2004) Synthesis of a silk-inspired peptide-oligothiophene conjugate. *Org. Biomol. Chem.* 2, 3541–3544.
- (64) Schillinger, E.-K., Mena-Osteritz, E., Hentschel, J., Börner, H. G., and Bäuerle, P. (2009) Oligothiophene versus β -sheet peptide: synthesis and self-assembly of an organic semiconductor-peptide hybrid. *Adv. Mater.* 21, 1562–1567.
- (65) Upton, T. G., Kashemirov, B. A., McKenna, C. E., Goodman, M. F., Prakash, G. K. S., Kultyshev, R., Batra, V. K., Shock, D. D., Pedersen, L. C., Beard, W. A., and Wilson, S. H. (2009) α,β -Difluoromethylene deoxynucleoside 5'-triphosphates: a convenient synthesis of useful probes for DNA polymerase β structure and function. *Org. Lett.* 11, 1883–1886.
- (66) Yamamoto, I., Sekine, M., and Hata, T. (1980) One-step synthesis of 5'-azido-nucleosides. *J. Chem. Soc., Perkin Trans. 1*, 306–310.
- (67) Rothmund, P. W. K. (2006) Folding DNA to create nanoscale shapes and patterns. *Nature* 440, 297–302.
- (68) Shih, W. M., Quispe, J. D., and Joyce, G. F. (2004) A 1.7-kilobase single-stranded DNA that folds into a nanoscale octahedron. *Nature* 427, 618–621.
- (69) Andersen, E. S., Dong, M., Nielsen, M. M., Jahn, K., Subramani, R., Mamdouh, W., Golas, M. M., Sander, B., Stark, H., Oliveira, C. L. P., Pedersen, J. S., Birkedal, V., Besenbacher, F., Gothelf, K. V., and Kjems, J. (2009) Self-assembly of a nanoscale DNA box with a controllable lid. *Nature* 459, 73–76.
- (70) Kuzuya, A., and Komiyama, M. (2009) Design and construction of a box-shaped 3D-DNA origami. *Chem. Commun.*, 4182–4184.
- (71) Dietz, H., Douglas, S. M., and Shih, W. M. (2009) Folding DNA into twisted and curved nanoscale shapes. *Science* 325, 725–730.
- (72) Douglas, S. M., Dietz, H., Liedl, T., Högberg, B., Graf, F., and Shih, W. M. (2009) Self-assembly of DNA into nanoscale three-dimensional shapes. *Nature* 459, 414–418.
- (73) Liedl, T., Högberg, B., Tytell, J., Ingber, D. E., and Shih, W. M. (2010) Self-assembly of three-dimensional prestressed tensegrity structures from DNA. *Nat. Nanotechnol.* 5, 520–524.
- (74) He, Y., Ye, T., Su, M., Zhang, C., Ribbe, A. E., Jiang, W., and Mao, C. (2008) Hierarchical self-assembly of DNA into symmetric supramolecular polyhedra. *Nature* 452, 198–201.
- (75) Ko, S. H., Su, M., Zhang, C., Ribbe, A. E., Jiang, W., and Mao, C. (2010) Synergistic self-assembly of RNA and DNA molecules. *Nat. Chem.* 2, 1050–1055.
- (76) Yang, H., McLaughlin, C. K., Aldaye, F. A., Hamblin, G. D., Rys, A. Z., Rouiller, I., and Sleiman, H. F. (2009) Metal–nucleic acid cages. *Nat. Chem.* 1, 390–396.
- (77) Aldaye, F. A., and Sleiman, H. F. (2007) Modular access to structurally switchable 3D discrete DNA assemblies. *J. Am. Chem. Soc.* 129, 13376–13377.
- (78) Aldaye, F. A., Palmer, A. L., and Sleiman, H. F. (2008) Assembling materials with DNA as the guide. *Science* 321, 1795–1799.
- (79) Aldaye, F. A., Lo, P. K., Karam, P., McLaughlin, C. K., Cosa, G., and Sleiman, H. F. (2009) Modular construction of DNA nanotubes of tunable geometry and single- or double-stranded character. *Nat. Nanotechnol.* 4, 349–352.
- (80) Lo, P. K., Karam, P., Aldaye, F. A., McLaughlin, C. K., Hamblin, G. D., Cosa, G., and Sleiman, H. F. (2010) Loading and selective release of cargo in DNA nanotubes with longitudinal variation. *Nat. Chem.* 2, 319–328.
- (81) McLaughlin, C. K., Hamblin, G. D., Aldaye, F. A., Yang, H., and Sleiman, H. F. (2011) A facile, modular and high yield method to assemble three-dimensional DNA structures. *Chem. Commun.* 47, 8925–8927.
- (82) Scheffler, M., Dorenbeck, A., Jordan, S., Wüstefeld, M., and von Kiedrowski, G. (1999) Self-assembly of trisiliconucleotidyls: the case for nano-acetylene and nano-cyclobutadiene. *Angew. Chem., Int. Ed.* 38, 3311–3315.
- (83) Zimmermann, J., Cebulla, M. P. J., Mönninghoff, S., and von Kiedrowski, G. (2008) Self-assembly of a DNA dodecahedron from 20 trisiliconucleotides with C_{3h} linkers. *Angew. Chem., Int. Ed.* 47, 3626–3630.
- (84) Chan, T. R., Hilgraf, R., Sharpless, K. B., and Fokin, V. V. (2004) Polytriazoles as copper(I)-stabilizing ligands in catalysis. *Org. Lett.* 6, 2853–2855.
- (85) Gottlieb, H. E., Kotlyar, V., and Nudelman, A. (1997) NMR chemical shifts of common laboratory solvents as trace impurities. *J. Org. Chem.* 62, 7512–7515.
- (86) Martin, R. B. (1996) Comparisons of indefinite self-association models. *Chem. Rev.* 96, 3043–3064.
- (87) Sun, H., Ye, K., Wang, C., Qi, H., Li, F., and Wang, Y. (2006) The π - π stacked geometries and association thermodynamics of quinacridone derivatives studied by ¹H NMR. *J. Phys. Chem. A* 110, 10750–10756.
- (88) Taboada, P., Attwood, D., Ruso, J. M., García, M., Sarmiento, F., and Mosquera, V. (2000) Self-association of the penicillin sodium nafillin in aqueous solution. *Langmuir* 16, 3175–3181.
- (89) Wang, M., Silva, G. L., and Armitage, B. A. (2000) DNA-templated formation of a helical cyanine dye J-aggregate. *J. Am. Chem. Soc.* 122, 9977–9986.
- (90) Yao, H., Domoto, K., Isohashi, T., and Kimura, K. (2005) In situ detection of birefringent mesoscopic H and J aggregates of thiocarbocyanine dye in solution. *Langmuir* 21, 1067–1073.
- (91) Kowalski, D., Kroeker, W. D., and Laskowski, M. (1976) Mung bean nuclease I. 6. Physical, chemical, and catalytic properties. *Biochemistry* 15, 4457–4463.
- (92) McCutchan, T., Hansen, J., Dame, J., and Mullins, J. (1984) Mung bean nuclease cleaves Plasmodium genomic DNA at sites before and after genes. *Science* 225, 625–628.
- (93) Seiders, T. J., Baldrige, K. K., Grube, G. H., and Siegel, J. S. (2001) Structure/energy correlation of bowl depth and inversion barrier in corannulene derivatives: combined experimental and quantum mechanical analysis. *J. Am. Chem. Soc.* 123, 517–525.
- (94) Mandelkern, M., Elias, J. G., Eden, D., and Crothers, D. M. (1981) The dimensions of DNA in solution. *J. Mol. Biol.* 152, 153–161.

(95) Watson, J. D., and Crick, F. H. C. (1953) Molecular structure of nucleic acids: a structure for deoxyribose nucleic acid. *Nature* 171, 737–738.

(96) Alonso, F., Moglie, Y., Radivoy, G., and Yus, M. (2009) Copper nanoparticles in click chemistry: an alternative catalytic system for the cycloaddition of terminal alkynes and azides. *Tetrahedron Lett.* 50, 2358–2362.

(97) Schmidt, L., Pedersen, E. B., Nielsen, C., Ivanov, C. B., Atanasova, R., Napoli, A., Sindona, G., Aksnes, D. W., and Francis, G. W. (1994) 5'-Azido and 5'-fluoro alpha-nucleosides as analogues of AZT and FLT. *Acta Chem. Scand.* 48, 215–221.

(98) Schmidt, M. W., Baldrige, K. K., Boatz, J. A., Elbert, S. T., Gordon, M. S., Jensen, J. H., Koseki, S., Matsunaga, N., Nguyen, K. A., Su, S., Windus, T. L., Dupuis, M., and Montgomery, J. A. (1993) General atomic and molecular electronic structure system. *J. Comput. Chem.* 14, 1347–1363.

(99) Rocha, G. B., Freire, R. O., Simas, A. M., and Stewart, J. J. P. (2006) RM1: A reparameterization of AM1 for H, C, N, O, P, S, F, Cl, Br, and I. *J. Comput. Chem.* 27, 1101–1111.